

Supplementary Information

Automatic detection of fluorescent droplets for droplet digital PCR: a device capable of processing multiple microscope images

Kaihao Mao,^{ab} Ye Tao,^{*b} Wenshang Guo,^{ab} Qisheng Yang,^b Meiyong Zhao,^{ab} Xiangyu Meng,^b Yinghao Zhang,^b and Yukun Ren^{*ab}

(* To whom correspondence should be addressed.)

a. State Key Laboratory of Robotics and System, Harbin Institute of Technology, Harbin 150001, P. R. China

b. School of Mechatronics Engineering, Harbin Institute of Technology, Harbin 150001, P. R. China

E-mail: taoyehit@hit.edu.cn (Ye Tao), rykhit@hit.edu.cn (Yukun Ren)

Table of contents

Supplementary Figures	1
Fig. S1. Microfluidic chip.	1
Fig. S2. Image brightness homogenization adjustment algorithm flow chart.	2
Fig. S3. Image contrast enhancement effect.	3
Fig. S4. Image lighting uneven removal effect.	4
Fig. S5. Inverted microscope image.	5
Fig. S6. Self-assembled microscope.	6
Fig. S7. Negative droplets have black outlines around the periphery.	7
Fig. S9. A-MMD.	9
Fig. S10. The size of the droplets before and after heating.	10
Fig. S11. A comparison of a 50 μm droplet with a 30 μm droplet.	11
Fig. S12. The recognition results of smaller droplets.	12
Supplementary Tables	13
Table S1. Filtering effect of LSCM images.	13
Table S2. Filtering effect of inverted microscope images.	13
Table S3. Filtering effect of self-assembled microscope images.	13
Table S4. Image brightness homogenization adjustment data sheet.	14
Table S5. Component parameters of the self-assembled microscope.	15
Table S7. The reaction system of λ DNA.	17
Table S8. Droplets count in LSCM images.	18
Table S9. Droplets count in inverted microscope images.	19
Table S10. Droplets count in self-assembled microscope images.	20
Table S11. Droplet counts at different template concentrations in LSCM images.	21
Table S12. Droplet counts at different template concentrations in inverted microscope images.	21
Table S13. Droplet counts at different template concentrations in self-assembled microscope images.	22
Table S14. The recognition rate of smaller droplets.	23
Table S15. A comparative evaluation of this work with reported methods.	24
Supplementary Notes	25
Note S1. Copy number calculation principle of ddPCR.	25
Note S2. Calculation principle of PSNR.	26
Supplementary References	27

Supplementary Figures

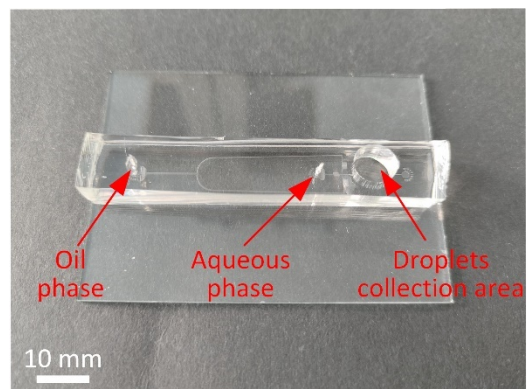


Fig. S1. Microfluidic chip.

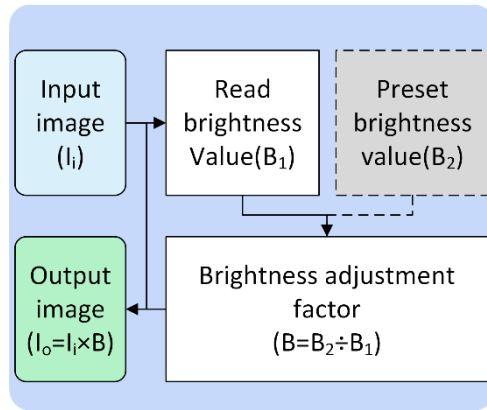


Fig. S2. Image brightness homogenization adjustment algorithm flow chart.

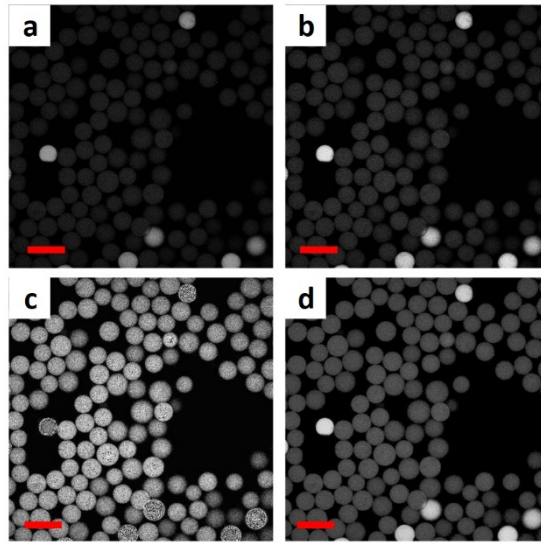


Fig. S3. Image contrast enhancement effect. (a) Original image. (b) Histogram normalization method. (c) Linear transformation method. (d) Piecewise linear transformation method. All scale bars represent 90 μm .

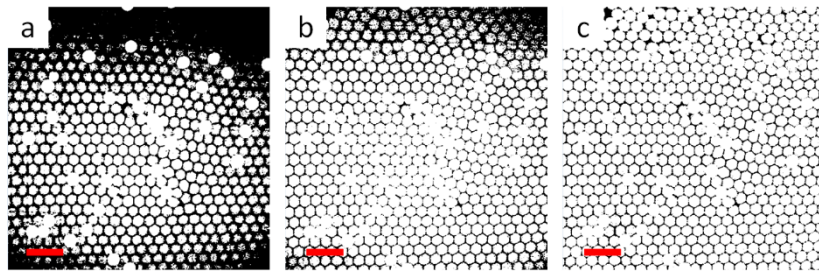


Fig. S4. Image lighting uneven removal effect. (a) Original image. (b) Global histogram equalization. (c) CLAHE. All scale bars represent 170 μm .

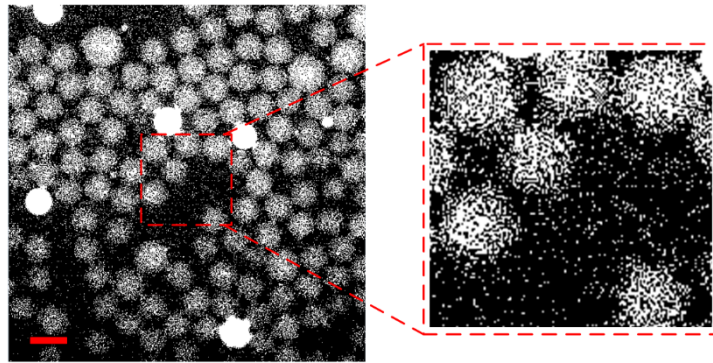


Fig. S5. Inverted microscope image. Scale bar represents 60 μm .

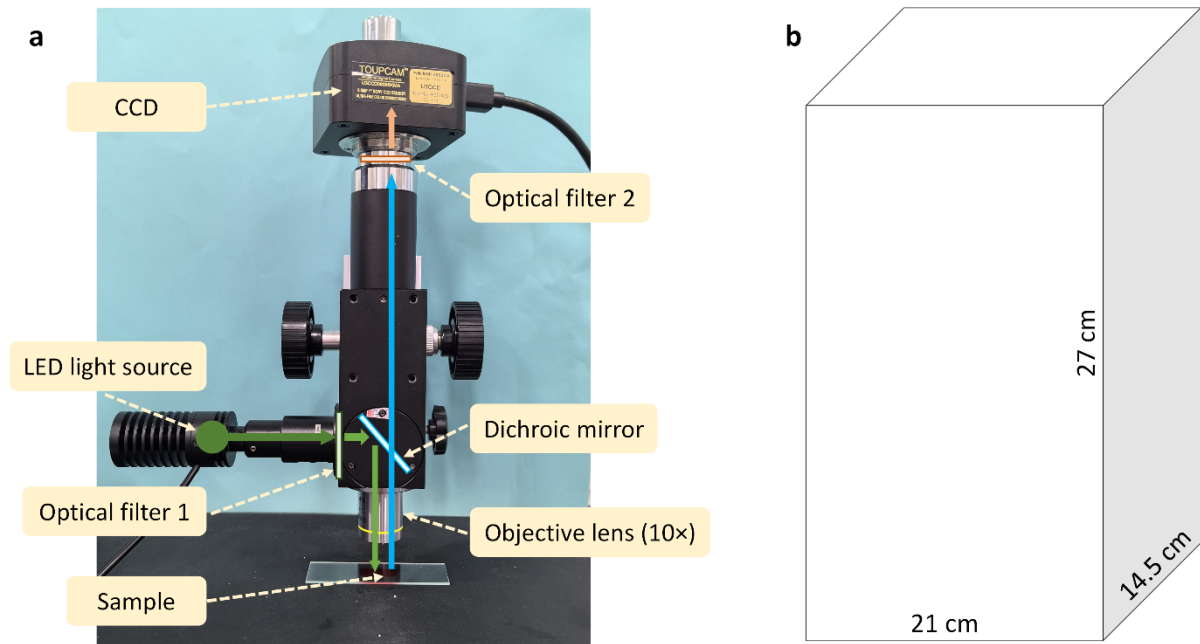


Fig. S6. Self-assembled microscope. (a) Microscope. (b) Microscope size.

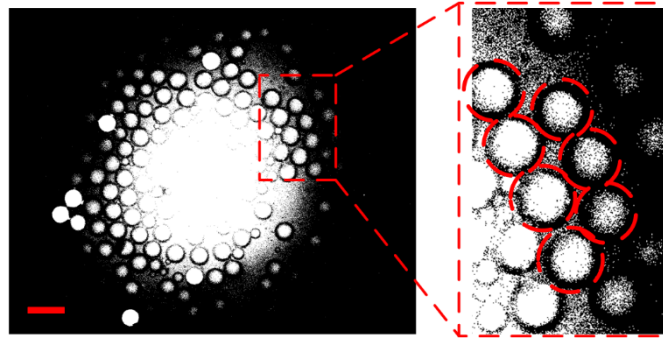


Fig. S7. Negative droplets have black outlines around the periphery. Scale bar represents 100 μm .

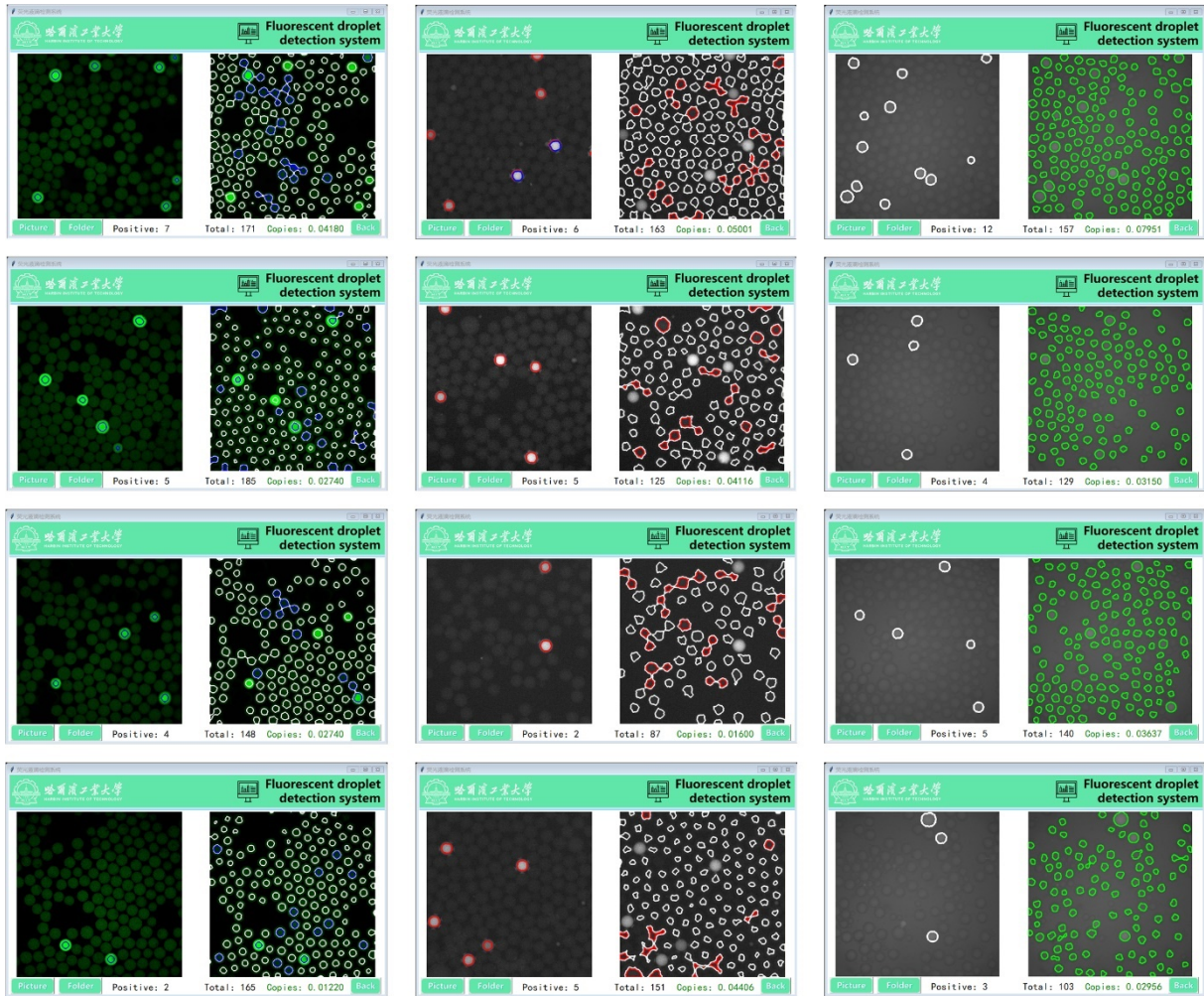


Fig. S8. Individual data analysis of multiple images.



Fig. S9. A-MMD. (a) Front view. (b) Rear view. (c) Size.

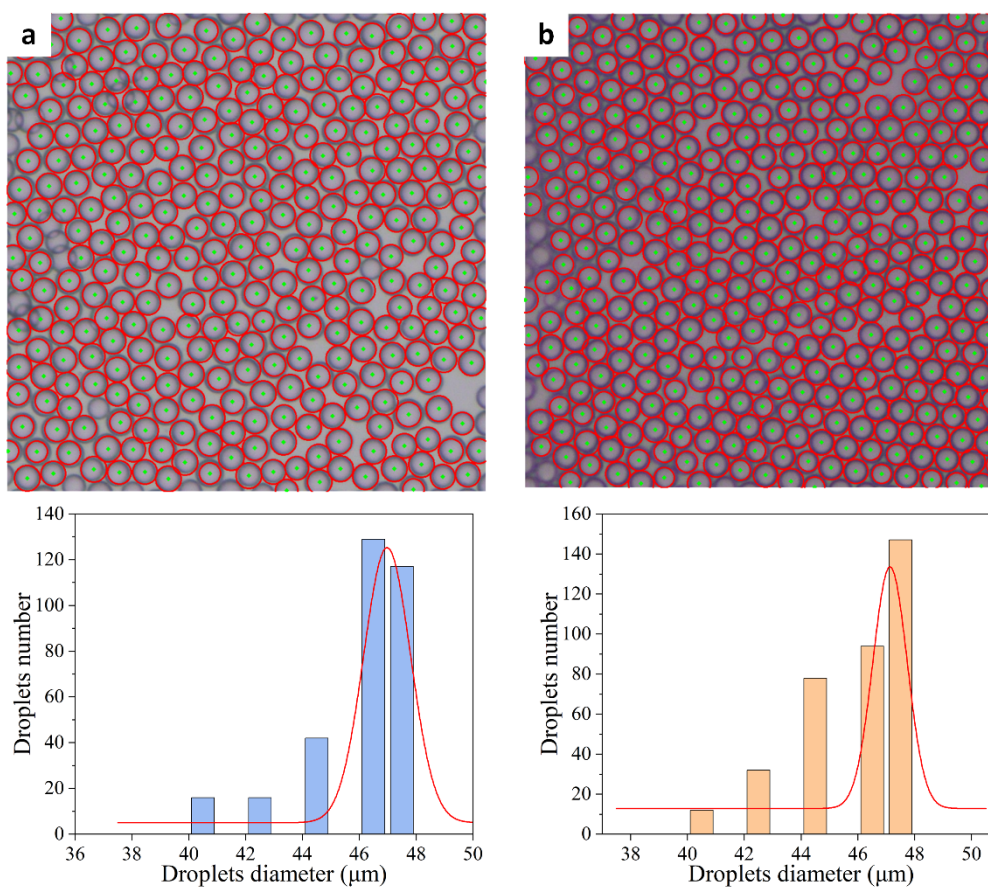


Fig. S10. The size of the droplets before and after heating. (a) Before heating. (b) After heating.

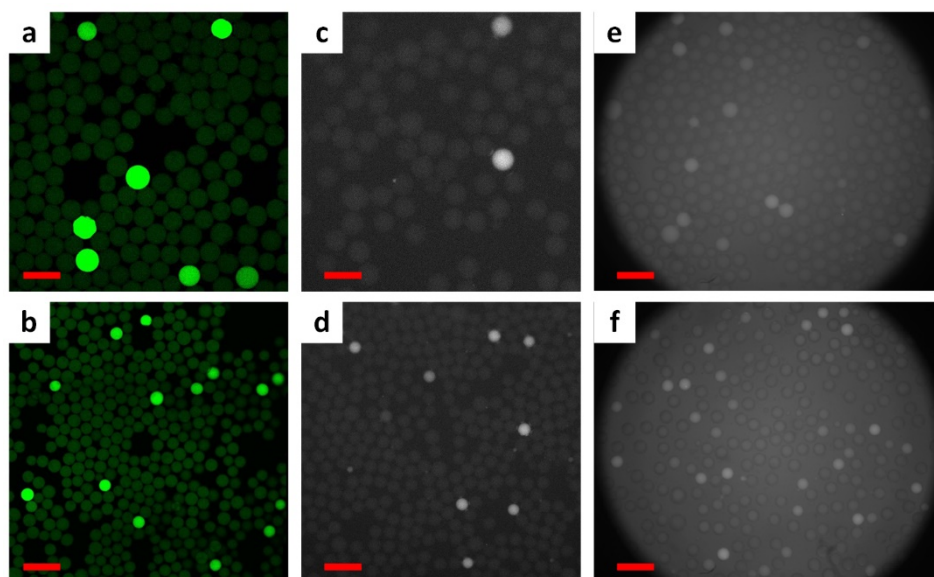


Fig. S11. A comparison of a 50 μm droplet with a 30 μm droplet. (a) LSCM image of 50 μm droplet. (b) Inverted microscope image of 50 μm droplet. (c) Self-assembled microscope image of 50 μm droplet. (d) LSCM image of 30 μm droplet. (e) Inverted microscope image of 30 μm droplet. (f) Self-assembled microscope image of 30 μm droplet. The scale bar of (a)-(d) represent 100 μm , the scale bars of (e)-(f) represent 120 μm .

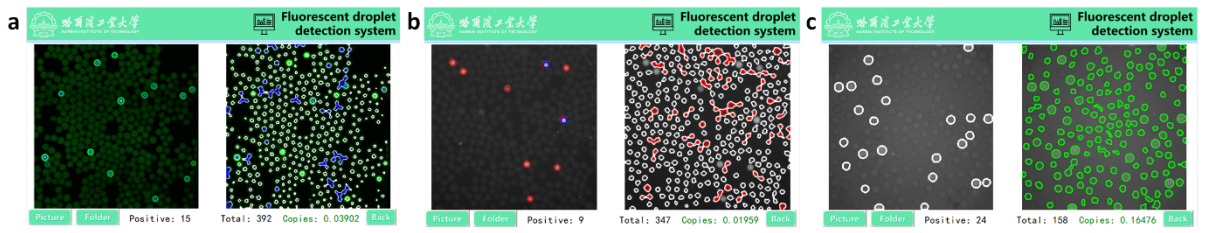


Fig. S12. The recognition results of smaller droplets. (a) LSCM image. (b) Inverted microscope image. (c) Self-assembled microscope image.

Supplementary Tables

Table S1. Filtering effect of LSCM images.

Filter mode	3 × 3	5 × 5	7 × 7
Mean filtering	25.54746476	25.64230698	25.42120857
Median filtering	27.75514209	27.63297067	27.46685074
Gaussian filtering	29.65851798	28.90407561	28.42273793

Table S2. Filtering effect of inverted microscope images.

Filter mode	3 × 3	5 × 5	7 × 7
Mean filtering	30.59914329	29.84477637	29.70253214
Median filtering	30.34942059	29.74993265	29.6950775
Gaussian filtering	32.47203564	31.05732404	30.35264612

Table S3. Filtering effect of self-assembled microscope images.

Filter mode	3 × 3	5 × 5	7 × 7
Mean filtering	40.80212	40.27384	40.14111
Median filtering	40.58522	40.16967	40.08713
Gaussian filtering	41.19436	40.7947	40.49261

Table S4. Image brightness homogenization adjustment data sheet.

Image sample	Before processing	After image processing	Error value	Error rate
1	28.617679	29.754558	0.04779	0.16%
2	20.974157	29.781216	0.026658	0.09%
3	11.145664	29.553978	0.227238	0.76%
4	22.974354	29.754801	0.200823	0.68%
5	22.454695	29.922881	0.16808	0.56%
6	22.887850	29.807311	0.11557	0.39%
7	22.877641	29.786519	0.020792	0.07%
8	52.477286	29.821069	0.03455	0.12%
9	36.569760	29.792437	0.028632	0.10%
10	29.627339	29.654027	0.13841	0.46%

The reference brightness value is 29.802348.

Table S5. Component parameters of the self-assembled microscope.

Part name	Correlation parameter
Sample	Excitation wavelength: 540 nm Emission wavelength: 560 nm
LED light source	Dominant wavelength: 535 nm Half-width: 30 nm Power: 12 W
Optical filter 1	Band pass filter 460-540 nm
Optical filter 2	Long wave pass filter 590 nm
Dichroic mirror	Type: long wave pass dichroic mirror Incidence Angle: 45° Reflection band: 500-535 nm Transmittance: 560-750 nm

Table S6. Specifications of the A-MMD.

Constituent	Specifications
Raspberry Pi 5	Random access memory 4 GB, internal storage 64 GB
HDMI display screen	7 inches, resolution 1024 × 600
Cooling fan	DC 5V, 24.5 mm × 24.5 mm × 14 mm
Device casing	3D printing materials PLA

Table S7. The reaction system of λ DNA.

Constituent	Volume (μ L)
Taq enzyme (5 U/ μ L)	0.5
10X PCR Buffer(Mg ²⁺ plus)	5
dNTP Mixture(each 2.5 mM)	4
λ DNA	0.5
297-R (10 μ M)	1.5
297-F (10 μ M)	1.5
SYTO 82	2.5
DNase/RNase-Free Water	34.5

Table S8. Droplets count in LSCM images.

Images	Positive droplets	Actual number	Recognition rate	Total droplets	Actual number	Recognition rate
1	34	34	100.00%	603	609	99.01%
2	34	34	100.00%	586	590	99.32%
3	32	32	100.00%	557	558	99.82%
4	6	6	100.00%	148	148	100.00%
5	5	5	100.00%	180	182	98.90%
6	4	4	100.00%	146	146	100.00%
7	1	1	100.00%	78	79	98.73%
8	7	7	100.00%	179	181	98.89%
9	7	7	100.00%	168	170	98.82%
10	2	2	100.00%	125	126	99.20%

The average recognition rate of all droplets is 99.27% and the standard deviation is 0.49%.

Table S9. Droplets count in inverted microscope images.

Images	Positive droplets	Actual number	Recognition rate	Total droplets	Actual number	Recognition rate
1	6	6	100.00%	173	176	98.30%
2	5	5	100.00%	157	161	97.52%
3	3	3	100.00%	141	141	100.00%
4	2	2	100.00%	87	87	100.00%
5	5	5	100.00%	148	152	97.37%
6	5	5	100.00%	133	133	100.00%
7	9	9	100.00%	361	361	100.00%
8	18	18	100.00%	635	640	99.22%
9	14	14	100.00%	562	574	97.91%
10	5	5	100.00%	145	146	99.32%

The average recognition rate of all droplets is 98.96% and the standard deviation is 1.09%.

Table S10. Droplets count in self-assembled microscope images.

Images	Positive droplets	Actual number	Recognition rate	Total droplets	Actual number	Recognition rate
1	11	11	100.00%	163	164	99.39%
2	4	4	100.00%	134	134	100.00%
3	12	12	100.00%	134	134	100.00%
4	5	5	100.00%	154	154	100.00%
5	4	4	100.00%	112	113	99.12%
6	3	3	100.00%	65	67	97.01%
7	6	6	100.00%	142	145	97.93%
8	2	2	100.00%	49	50	98.00%
9	2	2	100.00%	63	63	100.00%
10	5	5	100.00%	154	155	99.35%

The average recognition rate of all droplets is 99.08% and the standard deviation is 1.07%.

Table S11. Droplet counts at different template concentrations in LSCM images.

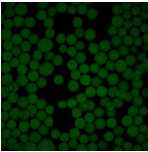
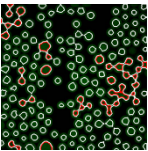
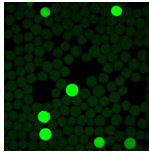
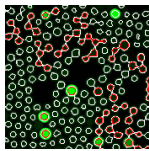
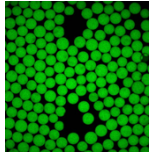
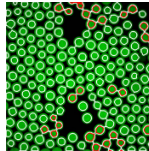
template concentrations	2×10^2 copies/ μL	2×10^3 copies/ μL	2×10^4 copies/ μL
Positive droplets	0	7	182
ImageJ	0	7	183
Recognition rate	100.00%	100.00%	99.45%
Total droplets	163	172	182
ImageJ	165	174	183
Recognition rate	98.79%	98.85%	99.45%
Image	 	 	 

Table S12. Droplet counts at different template concentrations in inverted microscope images.

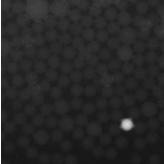
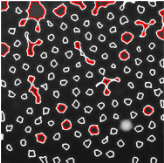
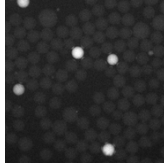
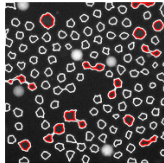
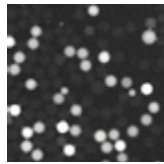
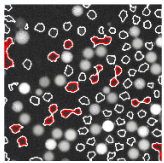
template concentrations	2×10^2 copies/ μL	2×10^3 copies/ μL	2×10^4 copies/ μL
Positive droplets	1	5	32
ImageJ	1	5	33
Recognition rate	100.00%	100.00%	96.97%
Total droplets	137	130	103
ImageJ	138	130	105
Recognition rate	99.28%	100.00%	98.10%
Image	 	 	 

Table S13. Droplet counts at different template concentrations in self-assembled microscope images.

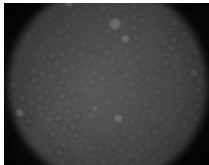
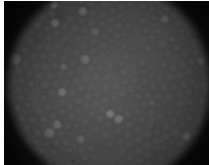
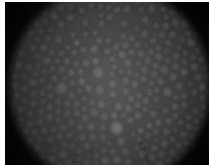
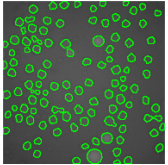
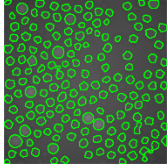
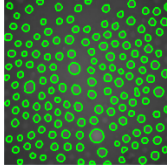
template concentrations	2×10^2 copies/ μL	2×10^3 copies/ μL	2×10^4 copies/ μL
Positive droplets	4	10	159
ImageJ	4	10	159
Recognition rate	100.00%	100.00%	100.00%
Total droplets	112	162	159
ImageJ	113	164	159
Recognition rate	99.12%	98.78%	100.00%
Image			
			

Table S14. The recognition rate of smaller droplets.

Type	Positive droplets	Actual number	Recognition rate	Total droplets	Actual number	Recognition rate
LSCM	15	15	100.00%	392	401	97.76%
Inverted microscope	9	9	100.00%	347	353	98.30%
Self-assembled microscope	24	23	95.83%	158	161	98.14%

Table S15. A comparative evaluation of this work with reported methods.

Methods	Positive recognition rate	Negative recognition rate	Total recognition rate
This work	100.00%	99.25%	99.27%
	100.00%	98.93%	98.96%
	100.00%	99.04%	99.08%
A quantitative image analysis method, Sensors, 2017 ¹	95.02%	-	95.86%
FluoroCellTrack, PLOS ONE, 2019 ²	-	-	92–99%
A deep learning-based high-throughput ddPCR droplet detection framework, Analyst, 2023 ³	99.71%	95.04%	-

Supplementary Notes

Note S1. Copy number calculation principle of ddPCR.

The calculation principle of the copy number in ddPCR is based on the Poisson distribution.⁴ Each droplet is a relatively independent area. For a designated droplet, the decision for a DNA molecule to enter this droplet is a binary choice, with entry recorded as 1 and non-entry as 0. Thus, for a specific droplet, if every DNA molecule makes the same choice, the event follows a binomial distribution (S1). Given the large number of droplets and the dilution of DNA molecules to a certain extent, it can be considered that the droplets approach infinity and the DNA molecules approach zero, then the DNA molecules contained in the droplets conform to the Poisson distribution (S2). When it is assumed that no DNA molecules enter the droplet, k is taken as zero at this point, yielding equation (S3). By taking the logarithm of both sides of equation (S3), the final copy number of the target DNA is obtained (S4).

$$P(x=k)=C_N^k p^k (1-p)^{N-k} \quad (S1)$$

$$p(x=k)=\frac{\lambda^k}{k!} e^{-\lambda} \quad (S2)$$

$$p(x=0)=1-\frac{m}{n}=e^{-\lambda} \quad (S3)$$

$$\lambda=-\ln\left(1-\frac{m}{n}\right) \quad (S4)$$

k : 0 or 1;

λ : DNA copy number in the drop;

d : the number of droplets generated;

x : if a destination DNA segment chooses whether to enter a droplet, then the probability of an entry event is $p=1/d$;

N : $N \times$ events have occurred;

P : the probability that the droplet contains k DNA molecules;

m : number of positive drops;

n : Total number of drops.

Note S2. Calculation principle of PSNR.

Peak Signal-to-Noise Ratio (PSNR) is a measure of the quality of an image after denoising or adding noise, with higher values indicating better filtering effects.⁵ In the context of images, it is used to evaluate the quality of two compared images, that is, the degree of distortion; the higher the PSNR, the less image distortion. The calculation formulas are shown as (S5) and (S6): first, calculate the Mean Squared Error (MSE), then calculate the PSNR, where MAX is taken as the maximum grayscale value of 255.

$$MSE = \frac{1}{mn} \sum_{i=0}^{m-1} \sum_{j=0}^{n-1} (I(i,j) - K(i,j))^2 \quad (S5)$$

$$PSNR = 10 * \log_{10} \left(\frac{MAX^2}{MSE} \right) \quad (S6)$$

$I(i, j)$: original image;

$K(i, j)$: image after noise removal;

m, n : size of image pixel value.

Supplementary References

1. R. F. Li, Y. B. Wang, H. Xu, B. W. Fei and B. J. Qin, *Sensors*, 2017, **17**, 13.
2. M. Vaithiyathan, N. Safa and A. T. Melvin, *PLoS One*, 2019, **14**, 22.
3. H. X. Yang, J. H. Yu, L. H. Jin, Y. P. Zhao, Q. Gao, C. R. Shi, L. Ye, D. Li, H. Yu and Y. K. Xu, *Analyst*, 2023, **148**, 239-247.
4. L. B. Pinheiro, V. A. Coleman, C. M. Hindson, J. Herrmann, B. J. Hindson, S. Bhat and K. R. Emslie, *Anal. Chem.*, 2012, **84**, 1003-1011.
5. C. Yim and A. C. Bovik, *IEEE Trans. Image Process.*, 2011, **20**, 88-98.